INFLUENCE OF NEUTRON RADIATION ON THE STABILITY OF THE ERYTHROCYTE MEMBRANE AND AN OXYHEMOGLOBIN FORMATION — PETKAU EFFECT STUDIES

Magdalena Kaczmarska[a], Iwona Habina[a]
Aleksandra Orzechowska[a], Katarzyna Niemiec-Murzyn[b]
Maria Fornal[c], Władysław Pohorecki[d], Krzysztof Matlak[e]
Józef Korecki[e], Tomasz Grodzicki[c], Květoslava Burda[a†]

[a]AGH University of Science and Technology
Faculty of Physics and Applied Computer Science
Department of Medical Physics and Biophysics, Kraków, Poland
[b]AGH University of Science and Technology
Multidisciplinary School of Engineering in Biomedicine, Kraków, Poland
[c]Jagiellonian University, Collegium Medicum
Department of Internal Medicine and Gerontology, Kraków, Poland
[d]AGH University of Science and Technology
Faculty of Energy and Fuels, Kraków, Poland
[e]AGH University of Science and Technology
Faculty of Physics and Computer Science
Department of Solid State Physics, Kraków, Poland

(Received November 17, 2015)

This paper examines the influence of a low dose of neutron radiation of 111 μGy (1.418 mSv — ICRP21, 1.277 mSv — ICRP74) on the stability of human red blood cells (RBCs). In the range of μGy doses, ionizing radiation may cause a serious oxidative stress in living organisms due to the Petkau effect. RBCs were chosen because their structure and function are well known, so they can be used as a model system for studying the influence of ionizing radiation on mammalian cell membranes. Atomic force microscopy (AFM) is applied to analyze the topography of RBCs, their shape and membrane-skeleton network, along with the Mössbauer spectroscopy to monitor different states of hemoglobin (Hb) and its ability to bind or release O_2 in untreated and irradiated erythrocytes. We find that neutron radiation at a dose of 111 μGy causes a shape change of RBCs and a stretching of the spectrin network. In addition, it modifies the permeability of erythrocyte membrane to gases and slows down the O_2 rebinding by Hb by a factor of 4 in comparison to untreated red cells. We also observe that a new form of Hb_{irr} occurs at a level of about 6%.

DOI:10.5506/APhysPolB.47.425

† Corresponding author: kvetoslava.burda@fis.agh.edu.pl

1. Introduction

Neutron radiation comes under the heading of indirectly ionizing radiation and is more penetrating than charged alpha, beta particles or γ-ray. Only in materials of low atomic number such as hydrogen, low energy γ-radiation is more penetrating than that of high energy neutrons. The energy transfer during neutron scattering could be very high, especially for hydrogen, in this case up to 100%. Hydrogen atoms are common in lipids, proteins and other biologically important structures of living organisms. Hydrogen nuclei produced during a collision with neutrons cause ionization of the biological material through which they travel. The formation of reactive oxygen species (ROS), for example singlet oxygen and free radicals, results in major damage to biomolecules. These harmful species and the products of their reactions have been shown to have dysfunctional effects in living cells [1, 2]. Neutrons indirectly involve high linear-energy transfer (high LET) radiation (protons, alphas, scattered ions) which significantly impairs the repair mechanisms of cells. Since it has a higher relative biological effectiveness (RBE) than γ- or beta-radiation by about 10 times, neutron therapy can be very effective. Usually, in radiotherapy fast neutrons are applied, *i.e.* those with energies higher than 20 MeV. The severity of the side effects depends on the total dose delivered and the general health of the patient.

Studies on the influence of low doses of neutron radiation at lower energy are required in order to better understand the action of neutrons on living organisms. There are only a few works available on this subject. In the case of high doses of ionizing radiation, at least 100 times higher than the estimated background radiation ($\sim$ 2.5 mGy at sea level), the severity of the cell damage is proportional to the dose and appears shortly after exposure [3]. However, cellular responses to doses absorbed at a low level cannot be extrapolated from these high doses. For doses from 5 mGy to 200 mGy, "radiation hormesis" and "radioadaptive responses" have been reported [4–6]. This is possible because stimulation of defensive mechanisms against ROS damage is to be expected. Most of them are the same as those activated under normal circumstances. The biological effects of these highly reactive compounds are controlled *in vivo* by a wide spectrum of antioxidant enzymatic mechanisms as, for example, by superoxide dismutases (SOD), glutathione peroxidase (GPx), catalases (CAT), peroxiredoxin, and also by such small antioxidant molecules as carotenoids, tocopherols, ascorbic acid and glutathione [7–13].

This work presents a study of the stability of RBCs exposed to neutron radiation at a dose of 111 μGy, which is about 3 orders of magnitude lower than those for which the radiation hormesis is observed. The phenomena expected were those associated with what is known as the Petkau effect, when an enhanced propagation of free radicals takes place [14, 15] as in

the case of RBCs treated with very low doses of γ-radiation [16]. Petkau showed that free radicals are more damaging to biological material in lower than higher concentrations because of the screening effect in the latter, when they more readily recombine with each other instead of interfering with the target molecules. This has non-monotonic consequences. We chose human RBCs because of their availability and their well-defined structure [17, 18]. The stability of erythrocytes exposed to neutron rays was monitored using absorption spectroscopy. Atomic force microscopy (AFM) was applied to investigate any modifications to the structure of irradiated RBC. This method is a powerful tool in studies of the erythrocyte membrane-skeleton [19] as well as other physico-chemical properties of RBCs [20]. The Mössbauer spectroscopy is usually used as a sensitive tool for the investigation of the valence and spin states of heme-iron and properties of its binding site in hemoglobin [21, 22]. In this work, it was also applied to monitor the permeability of the erythrocyte membrane to gases, and the reversibility of O_2 binding by hemoglobin in untreated and irradiated red cells [19]. This experimental approach allowed us to correlate changes in the RBC membrane-skeleton structure with hemoglobin's ability to bind or release O_2.

2. Materials and methods

RBCs were isolated from fresh blood. Heparin was added as an anticoagulant. Blood was taken from 3 healthy persons. The donors were non-smokers and had not undergone any therapy prior to the studies in at least the previous three months. They were free of any allergic diseases. The clinical characteristics and laboratory parameters of the healthy donors are presented in Table I. All morphological parameters remained in the physiological range.

Erythrocytes were isolated from blood using a standard method [20]. Blood was centrifuged at 4500 rpm at 4°C for 20 min and the pellet was collected. Then, the cells were suspended in a phosphate buffer (pH 7.4, NaH_2PO_4/Na_2HPO_4, 200 mM) and again centrifuged at 4500 rpm at 4°C. This procedure was repeated at least 3 times. Washed RBCs were suspended in a phosphate buffer at 4×10^9 red blood cells/ml. For the Mössbauer experiments, about 20-fold concentrated samples having a total volume of about 1.5 ml were used. These samples were kept frozen at -80°C. During the procedure of the isolation of erythrocytes and their further treatment with neutron radiation, samples were protected against light.

TABLE I

Clinical characteristics and laboratory parameters of studied donors. BPs — blood pressure [mmHg]. BPr — blood pressure [mmHg], Hb — hemoglobin [g/dl], Ht — hematocrit [%], RBC — red blood cells [mm^{-3}], MCV — mean corpuscular volume [fl], MCHC — mean corpuscular hemoglobin concentration [g/l], TCh — total cholesterol [mmol/l], LDL — low-density lipoprotein [mmol/l], HDL — high-density lipoprotein [mmol/l], TG — triglyceride [mmol/l], Gl — glucose [mmol/l], HbA_{1c} — glycated hemoglobin [%], Cr — creatinine [mol/l], Fib — fibrinogen [g/l], CRP — C-reactive protein [mg/l], TSH — thyroid-stimulating hormone [μlU/mL].

Patient	Healthy*
Sex	2M+1F
Age	25 ± 2.2
BPs	122.3 ± 1.9
BPr	77.7 ± 1.6
Hb	15.7 ± 0.2
Ht	46.1 ± 1.3
RBC	5.38 ± 0.17
MCV	85.8 ± 0.5
MCH	31.1 ± 1.9
TCh	4.9 ± 013
LDL	2.6 ± 0.3
HDL	1.63 ± 0.04
TG	1.02 ± 0.08
Gl	4.94 ± 0.13
HbA_{1c}	5.17 ± 0.13
Cr	83.3 ± 4.3
Fib	2.66 ± 0.26
CRP	3.36 ± 0.01
TSH	3.28 ± 0.5

*an average parameters are given for healthy donors; F — female, M — male.

^{239}Pu–Be was our source of neutron radiation. Neutron flux density in the sample position was 1.5×10^3 $n\mathrm{cm}^{-2}\mathrm{s}^{-1}$, which is equivalent to about 2.5 μGy/min or about 315 μSv/min — ICRP21 and 284 μSv/min — ICRP74. The contribution to energy deposition is as follows: protons 89.6%, alphas 0.5%, recoil ions and other high LET particles 8.5%, electron and photons only due to source neutrons interactions 1.3%. Dose due to photons from Pu–Be source (Pu fission products) activity of steel housing is less than 20% of total dose [23]. Neutron flux density and doses were calculated with the use of MCNP-6 code [24]. Neutron spectrum of Pu–Be source was taken from IAEA Compendium of Neutron Spectra and Detector Responses for Radiation Protection Purposes [25]. Energy deposition was calculated with the use of F6 tally and doses with the use of F4 tally modified

by standard dose function ICRP-21 1971 [26, 27] and ICRP-74 1996 ambient dose equivalent [28]. A sample was about 1 mm thick blood layer of about 1 g/cm^3 density and chemical composition taken from PNNL-15870 [29].

The hemolysis of RBCs was monitored using an absorption spectrometer (Varian Cary 50Bio). Samples were exposed to neutron rays for 45 min at room temperature. The rate dose of 2.5 μGy/min was constant. The supernatant, obtained from centrifuged non-irradiated or irradiated samples, was measured within wavelength range from 450 nm to 700 nm. The absorption spectra were fitted using the superposition of two Gaussian functions (three functions when a methemoglobin was present). The percentage of hemolysis was determined from the ratio of the area under the Gaussian curve with the absorption peak centered at 577 nm of an irradiated sample and a corresponding non-irradiated, totally hemolyzed sample. The spontaneous hemolysis of the control (untreated) sample was at a level of about 0.3% and this was always subtracted. All results were normalized to the amount of erythrocytes in the samples. Only freshly prepared RBCs were used.

Erythrocyte topography was detected using atomic force microscopy (AFM, Agilent 5500). About 200 μl of erythrocytes suspended in a phosphate buffer was placed on a mica surface (V5, Veeco). Measurements were carried out in air at room temperature, always 2 h after the sample's deposition on the mica. We did not use any of the chemicals which are usually applied in such experiments in order to stabilize the structure of erythrocytes. Measurements were performed in the contact mode. V-shaped Si_3N_4 cantilevers with a spring constant of 0.01 N/m were applied.

In the Mössbauer experiments, samples containing concentrated erythrocytes in the phosphate buffer were put in a home-made cryostat. The reversibility of O_2 binding to Hb was performed according to the procedure described in [22]. 50 mCi 57Co(Rh) was the source of the 14.4 keV γ-radiation. Measurements were performed at 85 ± 0.1 K. Experimental data were fitted using Recoil software [30]. The studies were approved by the Bioethics Committee of the Jagiellonian University (KBET/11/B/2009 and 124/KBL/OIL/2011).

3. Results and discussion

3.1. Erythrocyte topography

The applied 111 μGy dose of neutron radiation caused hemolysis of the erythrocytes at a level of $2 \pm 0.5\%$. This means that most of them remained unhemolized. Atomic force microscopy was applied to investigate differences in the shape and membrane structure between healthy RBCs both non-irradiated and irradiated. This method allows one to image the surfaces of biological cells with a nanometer resolution [22, 31, 32]. Because

the RBC membrane is only about 4 nm thick and the experiments were performed under partial dehydration of the samples, the cell membrane-skeleton network could be made visible. In Fig. 1, we present in the same resolution representative images of RBCs not irradiated (a) and those irradiated for 45 min with neutrons ((b) and (c)). The images in Fig. 1 (b) and (c) show two typical forms of erythrocytes for irradiated cells. In Fig. 1 (d), (e) and (f), there are three-dimensional pictures of the subsequent representative erythrocytes. One sees that RBC exposure to neutron radiation does not cause a change in cell size and, in some cases, even a biconcave shape is preserved (Fig. 1 (b)). However, all RBCs irradiated with neutrons have irregular craggy edges (Fig. 1 (b), (c), (e) and (f)). These changes are usually observed in erythrocytes suspended in a hypertonic medium [33].

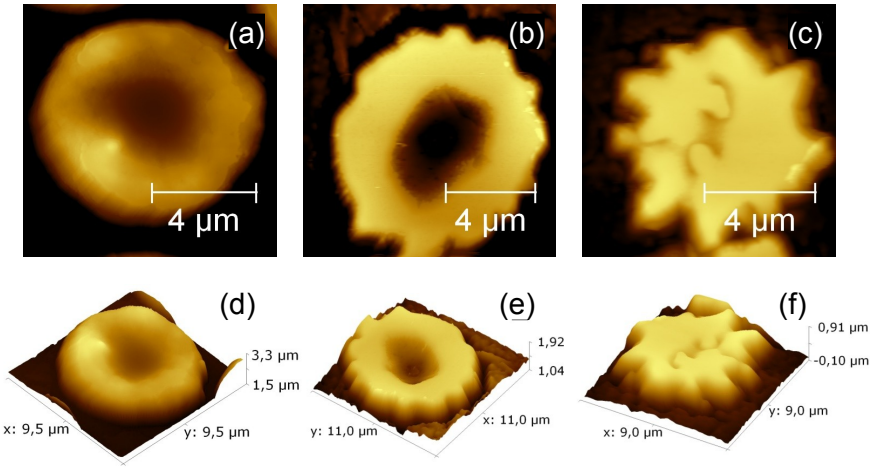

Fig. 1. AFM images of red blood cells isolated from a healthy donor: non-irradiated (a) and after 45 minutes of irradiation by neutron rays, the total deposited dose was 111 μGy ((b) and (c)); and their three dimensional counterparts: (d) — non-irradiated RBC, (e), (f) — irradiated RBCs.

The fine structures of the red cell membrane skeleton were monitored by scanning the surfaces of erythrocytes with a higher resolution, 2×2 μm^2 (Fig. 2 (a) and (b)). Elongated splits and protrusions are visible on the surface of the irradiated RBCs. Corresponding cross sections marked in Fig. 2 (a) and (b) are shown in Fig. 2 (c) and (d), respectively. Figure 2 (d) exposes both larger structures and finer structures. Usually, these occur in the case of irradiated erythrocytes. Distributions of protrusions and cavities for healthy non-irradiated and irradiated RBCs are presented in Fig. 3. Figure 3 (a), (b) show the distributions of fine protrusions on larger structures (Fig. 3 (c), (d)). The average values for each group of erythrocytes are given

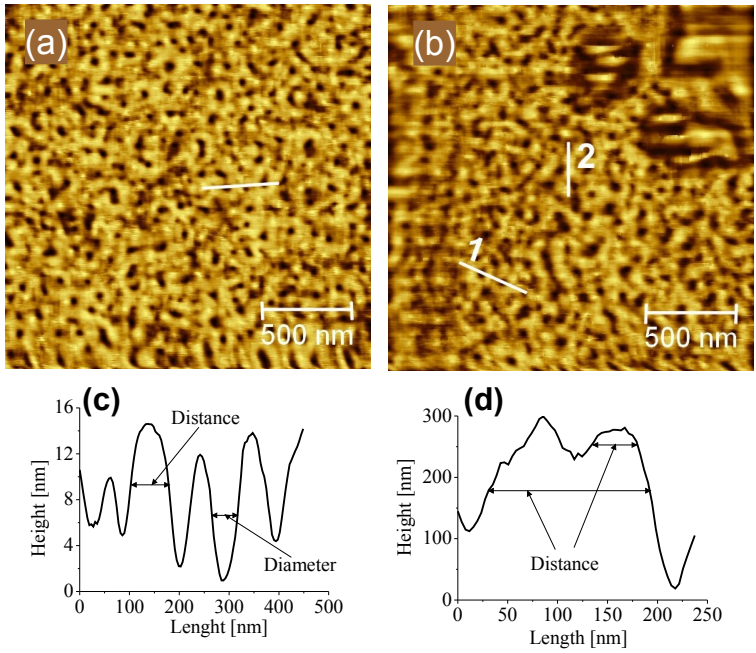

Fig. 2. AFM example images of the surfaces of healthy RBCs non-irradiated (a) and after irradiation by neutron rays at 111 μGy dose (b). The scan area is 2×2 μm^2. Cross sections along the directions indicated by white lines in (a) and (b) are shown in (c) and (d), for the cross section No. 2, respectively.

in the figures. Additionally, in Fig. 3 (e), (f) and (g), (h) diameters and lateral cross sections (shown as distances) are presented, respectively. Fine protrusions of about 38 ± 9 nm and longer structures of about 100 ± 20 nm, cavities about 39 ± 12 nm in diameter, and lateral cross sections of about 52 ± 18 nm characterize the honeycomb membrane skeleton of non-irradiated RBCs (Fig. 3 (a), (c), (e), (g)). In the case of irradiated RBCs, the membrane skeleton still has the honeycomb organization with cavities, large and small protrusions with average diameters of about 47 ± 15 nm, 52 ± 15 nm and 155 ± 31 nm, respectively (Fig. 3 (b), (d), (f)). These structures, as well as the lateral cross sections (62 ± 24 nm) seem to be larger in erythrocytes exposed to neutron radiation than in non-irradiated cells.

In order to extract possible differences between the membrane-skeleton organization in non-irradiated and irradiated healthy RBCs, statistical analysis of the data presented in Fig. 3 was carried out. All evaluations were done using a *t*-test for independent samples. If the assumption of normal distribution was fulfilled (it is the case of the large elongated protrusions), a parametric *t*-test was used, otherwise (all other data) a non-parametric Mann–Whitney U-test was applied.

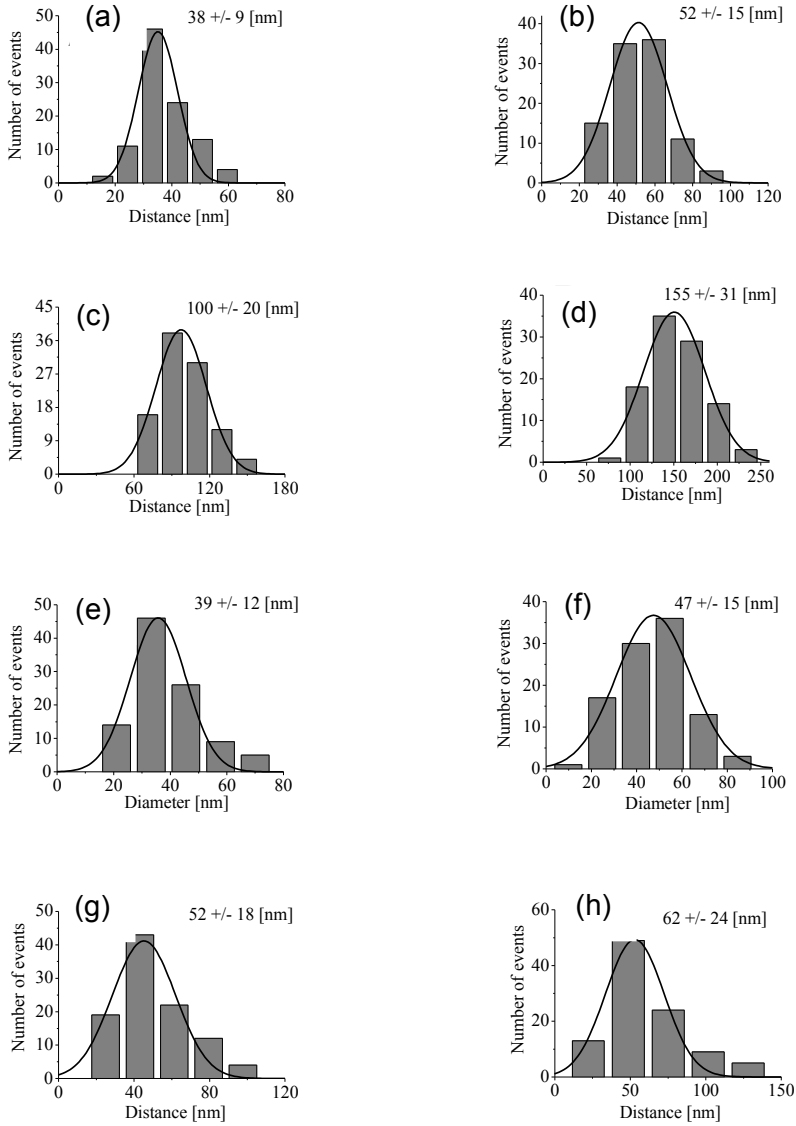

Fig. 3. Gaussian distributions of the sizes of fine protrusions (a), (b), of large protrusions (c), (d) and of cavity diameters (e), (f) as well as of protrusions (g), (h) along lateral cross sections (for example, see line 1 in Fig. 2 (b)) are presented for the control and irradiated RBCs in the left and right panel, respectively. The estimated average values are given in the corresponding diagrams. In each case, above 100 structures were taken into account.

The statistical analysis shows that there are significant differences between the corresponding data sets obtained for the non-irradiated and irradiated red cell structures at a level of $p \leq 0.01$. A comparison of the mean values for these two data sets is presented in Fig. 4 as box and whisker plots.

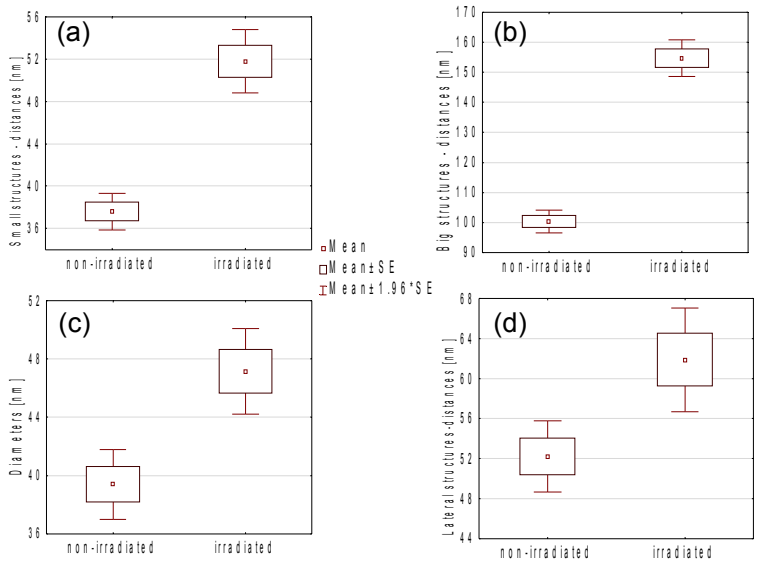

Fig. 4. Quantitative analysis of differences between the subsequent structures of erythrocyte membrane skeleton of non-irradiated and irradiated RBCs from healthy donors. The dose of neutron radiation applied was 111 μGy. The size differences of fine protrusions, large protrusions, diameters of cavities and protrusions along lateral cross sections are shown in figures (a), (b), (c) and (d), respectively.

The RBC membrane composed of cholesterol and phospholipids is spread over an elastic network of skeletal proteins via transmembrane peptides [18, 34]. It has been shown that the network of short actin filaments is cross-linked into a hexagonal structure by 200 nm long, flexible spectrin tetramers. The lengths of the short actin filaments containing approximately 13 monomers at the central junctions are stabilized and limited by association with rodlike tropomyosin molecules (about 33–34 nm long) and the tropomyosin-binding protein, tropomodulin (14.5 ± 2.4 nm in diameter) [35, 36]. Spectrin is also associated with ankyrin, and the distance from the tail end of spectrin to its ankyrin binding site is about 78 ± 7 nm as the spectrin dimmer is estimated to be 100 nm long [37]. Due to these interactions, the skeleton network forms tetra-, penta-, hexa- or heptagonal structures. Analysis of the present structures shows that this honeycomb pattern indeed represents the membrane-skeleton network but one has to take into

account that the sizes of the structures obtained from cross sectional profiles are somewhat exaggerated [32, 38]. However, this overestimation should not exceed about 20%. On the other hand, under these experimental conditions, unstretched skeleton molecules are monitored. Spectrin tetramers may, therefore, have a length of about 1/3 of their stretched conformation [38] and that is why the fine protrusions (of about 38–52 nm) can be assigned to such spectrins or to junctional/ankyrin complexes [32, 35, 36, 39]. The larger protrusions of about 100–155 nm correspond to partially stretched tetrameric spectrin molecules.

These changes in shape and in membrane-skeleton organization in RBCs exposed to a neutron radiation dose as low as 111 μGy provide experimental evidence for the Petkau effect. So far, morphological changes in human erythrocytes were reported for much higher ($> 10^6$ order of magnitude) doses of thermal neutrons (flux 9.4×10^9 neutrons/s cm^2 corresponding to a dose rate of 83 mGy/min), up to 72 Gy [40]. The authors detected a four-stage discoid-to-spheroid shape transformation of damaged RBCs using scanning electron microscopy. An irregular RBC shape and aggregation of cells due to ROS action on the erythrocyte membrane were also observed for rat erythrocytes exposed to fast neutrons at the dose of 0.1 mGy (1.0 mSv) and for murine RBCs irradiated by neutrons and concomitant γ-radiation at a total dose of 0.5–14 Gy [41, 42]. Irradiated RBCs had increased osmotic fragility which was related most probably to their morphological modifications.

Usually, effects like those which cause the destruction of RBCs are reported for much higher doses and dose rates of ionizing radiation [43–48]. Protein–SH groups have been shown to be especially sensitive to oxidative stress [49]. However, lipids are most probably the first target of ROS action, given that Petkau proved that lipid peroxidation occurs even under conditions of background radiation [3, 14, 50, 51].

3.2. Mössbauer measurements

Neutron radiation is the most penetrating radiation and it can also modify the inner structures of RBCs. In particular, this study found that neutron doses as low as 111 μGy caused oxyhemoglobin (OxyHb) and deoxyhemoglobin (DeoxyHb) to change into a new form called Hb_{irr}, which is characterized by a low isomer shift (IS) of about 0.20 mm/s and low quadrupole splitting (QS) of about 0.35 mm/s [52]. The results also show that OxyHb may turn into $HbOH/H_2O$, which is resistant to the action of neutrons under our experimental conditions. Interestingly, the hyperfine parameters of the new Hb_{irr} state detected in erythrocytes exposed to 1.8 mGy γ-radiation differ from those estimated in the case of RBCs irradiated by neutrons. They were more similar to MetHb parameters (IS $\approx$ 0.07 mm/s and QS $\approx$ 0.47 mm/s), which suggests a five coordinated heme-iron in a

high spin oxidized state [16]. However, the hyperfine parameters found for Hb_{irr} in erythrocytes irradiated by neutrons are rather close to those usually observed for a low spin ferrous state [21, 53] although Fe^{3+} in a strong electric field with almost spherical symmetry, which could be formed due to histidine (His) imidazole ring radiolysis, cannot be excluded [52, 54].

Recently, it has been shown that the Mössbauer spectroscopy can be used in monitoring oxygen rebinding by Hb inside RBCs [22]. The same experimental protocol is applied here to check how the above described morphological changes in RBCs caused by the influence of neutrons on gas exchange through the erythrocyte membrane and the affinity of Hb to O_2 binding. Example Mössbauer spectra of two samples collected at different times after incubation under low O_2 (high N_2) pressure are shown in Fig. 5. Figure 6 (a) and (b) shows the time-evolution of OxyHb formation after the RBC transfer to low N_2 (high O_2) pressure and other Hb forms present in red cells non-irradiated and irradiated with neutrons (111 μGy).

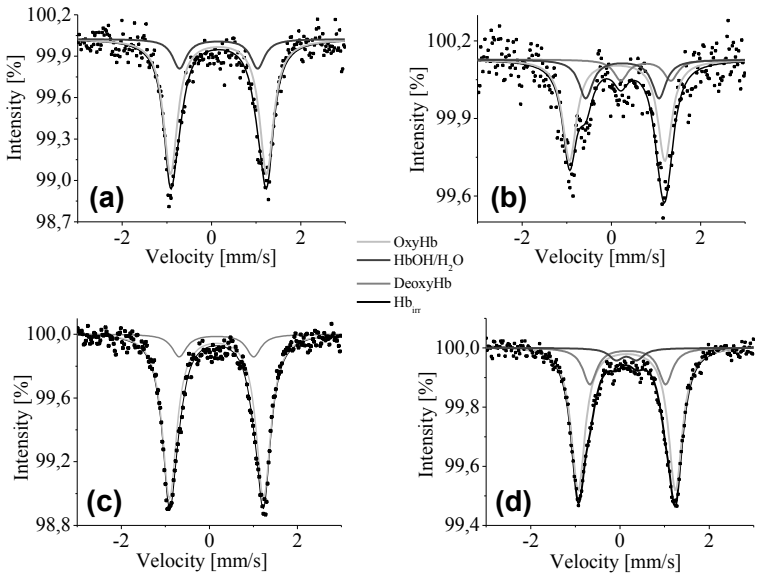

Fig. 5. Example Mössbauer spectra of Hb states in healthy RBCs non-irradiated (a), (b) and after irradiation (c), (d) with 111 μGy neutron rays ((a), (c) — sample 1; (b), (d) — sample 2) measured at 85 K under low N_2 pressure conditions and collected about 7 h (a), (b), 25 h (c) and 72 h (d) after transfer of the samples from high N_2 (low O_2) pressure conditions at room temperature ($T = 296 \pm 1$ K) to low N_2 (high O_2) pressure conditions at 85 K. Both samples were obtained from one donor during the same isolation procedure. Lower effects of the Mössbauer spectra measured for the irradiated sample are caused by the partial loss of experimental material due to the irradiation and additional centrifugation.

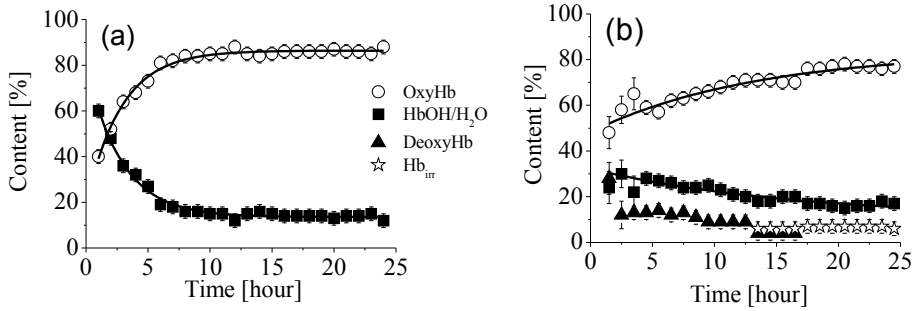

Fig. 6. Time-dependent changes in the contribution of $HbOH/H_2O$ and OxyHb for non-irradiated (a) and irradiated (b) RBCs. In the case of the irradiated sample, contributions of two other Hb states (DeoxyHb and Hb_{irr}) are shown.

The Mössbauer spectra of untreated RBCs can be decomposed into two subspectra characterized by different hyperfine parameters. The subspectrum with the largest QS of about 2.17 mm/s is characteristic for a diamagnetic state in OxyHb [21]. The doublet with QS $\approx$ 1.70 mm/s is assigned to deoxyhemoglobin in which the OH/H_2O molecule is the 6^{th} ligand of the heme-iron ($HbOH/H_2O$). In this case, the heme-iron could be in a mixed valence state (Fe^{2+}/Fe^{3+}) with mixed spin states [21]. In the case of the irradiated sample, a third component with IS $= 0.77 \pm 0.14$ mm/s and QS $= 1.12 \pm 0.26$ mm/s arises most probably from modified DeoxyHb, in which the heme-iron is present in a high spin Fe^{2+} state. However, in DeoxyHb as usually observed, QS is about two times larger [21, 53]. The quadrupole splitting for this Hb state increases up to about 2.0 mm/s with increasing time of measurements (data not shown, only the contribution of this DeoxyHb is presented in Fig. 6) and that is why it is ascribed to DeoxyHb. After 72 hours, there was no more DeoxyHb in the Mössbauer spectra. Instead, the Hb_{irr} content increased (IS $= 0.15 \pm 0.09$ mm/s and QS $= 0.46 \pm 0.14$ mm/s). The same changed Hb_{irr} state was already visible after 13.5 h (Fig. 6).

In non-irradiated RBCs, the content of $HbOH/H_2O$, which was initially (after 1 h) at a level of about 60%, diminishes with a half-life time $\sim$ 2 h reaching a stable level of about 18% after $\sim$ 8 h. Then, it remains constant to the final measurement. At the same time, the content of OxyHb increases from an initial level of about 40% to 85% after 8 h of measurement. Reversible oxygen binding by hemoglobin from irradiated RBCs in comparison to the non-irradiated RBCs slows down significantly. The half-life time of the changes in the contribution of OxyHb and $HbOH/H_2O$ increases by almost 4 times up to $\sim$ 10 h.

These results show for the first time that due to the Petkau effect, a new form of Hb occurred inside irradiated RBCs, and that modifications of the erythrocyte membrane result in a decreased rate of oxygen rebinding by Hb. Because in the Mössabuer experiments an increase in time is related to increased oxygen partial pressure, one may conclude that the Hb affinity to bind O_2 decreases and that the saturation of OxyHb is shifted towards higher oxygen partial pressure in irradiated RBCs.

4. Conclusions

The main outcome of this paper is experimental evidence that neutron radiation at as small dose as ~ 100 μGy causes changes in RBCs including modifications in the structural and functional properties of erythrocytes: *(i)* in their shape and membrane skeleton network and *(ii)* in the affinity of Hb to oxygen. All these changes can be explained by the Petkau effect.

It may be stated more precisely that:

1. Topography measurements using AFM reveal changes in the shape of irradiated RBCs, characteristic of erythrocytes in a hypertonic environment. These changes are related to the fact that the membrane skeleton is less tense. A more stretched spectrin network than in non-irradiated RBCs is most probably responsible directly or indirectly for the disruption of RBC membrane permeability to water molecules.

2. Mössbauer studies of O_2 rebinding by Hb inside RBCs show that this small neutron irradiation causes a decrease in the affinity of Hb to oxygen binding. This phenomenon may also be related to morphological changes in irradiated erythrocytes because the interaction of deoxyHb with membrane-skeleton proteins may regulate it [55–57]. In addition, gaseous exchange via the RBC membrane may be impaired.

3. A new form of Hb_{irr} is detected in the Mössabuer spectra of irradiated RBCs. It has previously been reported that only two physiologically active Hb forms (OxyHb and DeoxyHb) are sensitive to such low doses of neutron radiation [52].

The results obtained from these studies of the Petkau effect in RBCs irradiated by neutrons at very low doses may help us to understand hormesis and what is known as the "by-stander" effects observed at much higher doses of ionizing radiation [2, 58–60] and develop new radiological approaches which will reduce the side effects of irradiation.

This work was partially supported by a grant from the Polish Ministry of Science and Higher Education N N402 471337 (2009–2012), a doctoral grant from WFiIS AGH University of Science and Technology, Kraków and a grant from the Polish National Center of Science 2011/01/N/NZ5/00919 (2011–2013).

REFERENCES

[1] A. Berroud, A. Le Roy, P. Voisin, *R. Environ. Biophys.* **35**, 289 (1996).
[2] B. Jayashree, T.P.A. Devasagayam, P.C. Kesavan, *Current Sci.* **80**, 515 (2001).
[3] L. De Saint-Georges, *J. Biol. Reg. Homeos. Ag.* **18**, 96 (2004).
[4] E.J. Calabrese, L.A. Baldwin, *Nature* **421**, 691 (2003).
[5] L.E. Feinendegen, *Brit. J. Radiol.* **78**, 3 (2005).
[6] B.L. Cohen, *J. Amer. Phys. Surgery* **13**, 70 (2008).
[7] A. Meister, *J. Biol. Chem.* **269**, 9397 (1994).
[8] J. Bannister, W. Bannister, G. Rotilio, *CRC Cr. Rev. Bioch.* **22**, 111 (1987).
[9] F. Johnson, C. Giulivi, *Mol. Aspects of Med.* **26**, 340 (2005).
[10] P. Chelikani, I. Fita, P. Loewen, *Cell. Mol. Life Sci.* **61**, 192 (2004).
[11] S. Padayatty *et al.*, *J. Amer. Coll. Nutri.* **22**, 18 (2003).
[12] K. Bagchi, S. Puri, *East. Mediter. Health J.* **4**, 350 (1998).
[13] H. Sies, W. Stahl, *Am. J. Clin. Nutr.* **62**, 1315S (1995).
[14] A. Petkau, *Health Phys.* **22**, 239 (1972).
[15] R. Graeub, *Petkau Effect, the Devasting Effect of Nuclear Radiation on Human Health and the Environment*, 2nd Edn., Four Walls Eight Windows, New York 1994.
[16] M. Kaczmarska *et al.*, *Acta Biochim. Pol.* **58**, 489 (2011).
[17] E.M. Pasini *et al.*, *Blood* **108**, 791 (2006).
[18] W.A. Anong *et al.*, *Blood* **114**, 1904 (2009).
[19] M. Kaczmarska *et al.*, *Cell Biochem. Biophys.* **67**, 1089 (2013).
[20] K. Burda *et al.*, *Appl. Organomet. Chem.* **16**, 148 (2002).
[21] G. Lang, W. Marshall, *Proc. Phys. Soc.* **87**, 3 (1966).
[22] K. Burda *et al.*, *Biochim. Biophys. Acta* **1244**, 345 (1995).
[23] S. Mayer, T. Otto, N. Golnik, Determination of the Photon-Contribution of a ^{238}Pu–Be Source, Divisional Report CERN-TIS-2002-014-RP-CF, p. 8, 2002.
[24] J.T. Goorley *et al.*, Initial MCNP6 Release Overview — MCNP6 version 1.0, LA-UR-13-22934, p. 42, 2013.

[25] Technical Reports Series No. 403, Compendium of Neutron Spectra and Detector Responses for Radiation Protection Purposes, 2001; Supplement to Technical Reports Series No. 318, International Atomic Energy Agency, Vienna, p. 337.

[26] ICRP-21, International Commission on Radiological Protection, Pergamon Press, April 1971.

[27] ICRP Committee 3 Task Group, P. Grande, M.C. O'Riordan, chairmen, Data for Protection Against Ionizing Radiation from External Sources: Supplement to ICRP Publication 15, 1971.

[28] ICRP, Conversion Coefficients for Use in Radiological Protection Against External Radiation, ICRP Publication 74. Ann. ICRP 26 (3–4), 1996.

[29] R.J. McConn Jr *et al.*, March 2011. Compendium of Material Composition Data for Radiation Transport Modeling, 29 Blood (ICRP) PIET43741-TM-963, PNNL-15870 Rev. 1, pp. 41–42.

[30] D.G. Rancourt, J.-Y. Ping, *Nucl. Instrum. Methods B* **58**, 85 (1991).

[31] M. Takeuchi *et al.*, *Biophys. J.* **74**, 2171 (1998).

[32] R. Nowakowski, P. Luckham, P. Winlove, *Biochim. Biophys. Acta* **1514**, 170 (2001).

[33] M. Girasole, S. Dinarelli, G. Boumis, *Micron* **43**, 1273 (2012).

[34] J. Liu *et al.*, *Blood* **115**, 2021 (2010).

[35] J.A. Ursitti, V.M. Fowler, *J. Cell Sci.* **107**, 1633 (1994).

[36] V. Bennett, *Biochim. Biophys. Acta* **988**, 107 (1989).

[37] P.R. Stabach *et al.*, *Blood* **113**, 5377 (2009).

[38] A.H. Swihart, J.M. Mikrut, J.B. Ketterson, R.C. MacDonald, *J. Microsc.* **204**, 212 (2001).

[39] S.C. Liu, L.H. Derick, J. Palek, *J. Cell. Biol.* **104**, 527 (1987).

[40] A.C. Nelson, H.R. Wyle, *Scanning Electron Microscopy J.* **IV**, 1623 (1985).

[41] M.A. Fadel, S.I. Hosam, S.A. Eman, *Rom. J. Biophys.* **21**, 27 (2011).

[42] T. Kubasova, S. Antal, Z. Somosy, G.J. Köteles, *Radiat. Environ. Biophys.* **23**, 269 (1984).

[43] B. Shapiro, G. Kollmann, *Radiat. Res.* **34**, 335 (1968).

[44] G. Kollmann, B. Shapiro, D. Martin, *Radiat. Res.* **37**, 551 (1969).

[45] S. Yonei, M. Kato, *Radiat. Res.* **75**, 31 (1978).

[46] A.W.T. Konings, *Int. J. Radiat. Biol.* **40**, 441 (1981).

[47] J.C. Edwards, D. Chapman, W.A. Cramp, M.B. Yatvin, *Prog. Biophys. Mol. Biol.* **43**, 71 (1984).

[48] W. Leyko, G. Bartosz, *Int. J. Radiat. Biol.* **49**, 743 (1986).

[49] D. Tsun-Yee Chiu, T.Z. Liu, *J. Biomedical Sci.* **4**, 256 (1997).

[50] A. Petkau, W.S. Chelack, *Biochim. Biophys. Acta* **433**, 445 (1976).

[51] J.A. Raleigh, W. Kremers, B. Gaboury, *Int. J. Radiat. Biol.* **31**, 203 (1977).

[52] K. Niemiec *et al.*, *Hyperfine Interact.* **206**, 95 (2012).
[53] H. Chen, M. Ikeda-Saiko, S. Shoik, *J. Amer. Chem. Soc.* **30**, 14778 (2008).
[54] D. Rhynard, G. Lang, K. Spartalian, T. Yonetani, *J. Chem. Phys.* **71**, 3715 (1979).
[55] J.A. Walder *et al.*, *J. Biol. Chem.* **259**, 10238 (1984).
[56] G. Chetrite, R. Cassoly, *J. Mol. Biol.* **185**, 639 (1985).
[57] H. Chu, *et al.*, *Blood* **111**, 932 (2008).
[58] K. Yamaoka *et al.*, *J. Radiat. Res.* **45**, 89 (2004).
[59] T. Kataoka *et al.*, *J. Radiat. Res.* **48**, 505 (2007).
[60] A. Otani *et al.*, *Amer. J. Pathology* **180**, 328 (2012).